ISSN: 2093-5374 / E-ISSN: 2093-5382

Classification of Lung Diseases Using a Federated Proximal Term-based Two-Layer LSTM with Federated Learning and Blockchain

Parikshith Nayaka Sheetakallu Krishnaiah[1*], and Dr.N. Dayanand Lal[2]

[1*]Research Scholar & Assistant Professor, Department of CSE, GITAM School of Technology, Bengaluru, Karnataka, India. npariksh@gitam.edu, https://orcid.org/0000-0001-9325-7363

[2]Assistant Professor, Department of CSE, GITAM School of Technology, GITAM (Deemed to be University), Nagadenahalli, Doddabalapura, Bengaluru, India. dnarayan@gitam.edu, https://orcid.org/0000-0003-3485-9481

Received: October 30, 2024; Revised: December 15, 2024; Accepted: January 24, 2025; Published: March 31, 2025

Abstract

In recent years, automated discovery of thoracic diseases from Chest X-ray images (CXR) has become an essential field of computer-aided analysis. The diversity and scarcity of medical data make it complex to generate a precise global classification in the healthcare sector. The main reasons are privacy issues and legal obstacles limiting data sharing between healthcare institutions. On the contrary, data from a single source is hardly enough for developing a universal analysis model. Therefore, Federated Learning (FL) is a potential solution for data diversity and privacy issues. This research uses the FL approach to effectively learn from multiclass and heterogeneous medical data. However, the FL approach is susceptible to adversarial attacks; therefore, blockchain (BC) is integrated to enhance the security and privacy of patient data. This paper proposes the aggregator model, i.e., two-layer Long Short-Term Memory (2LLSTM) with the federated proximal term (FedProx), namely 2LLSTMFP, for enhancing the classification. The proximal term integrated with the 2LLSTM solves the issues created by data heterogeneity and increases stability during classification.

2LLSTMFP aggregates the classified information from the Convolutional Neural Network (CNN). The incorporated FP term develops the utilisation of proximal operators to update 2LLSTMFP weights regularly. The updated 2LLSTMFP weights regularise the effect of adversarial updates with BC, which further improves its robustness to malicious devices, i.e., adversarial attacks. The developed FLBC-2LLSTMFP is evaluated by using the ChestX-ray14 dataset. The FLBC-2LLSTMFP is analysed regarding accuracy, specificity, precision, recall, F1-score, False Positive Rate (FPR), and False Negative Rate (FNR). The existing research MobileLungNetV2 and MLRFNet are used to compare with the FLBC-2LLSTMFP. The accuracy of FLBC-2LLSTMFP is 99.98%, which is higher than that of MobileLungNetV2 and MLRFNet.

Keywords: Blockchain, Chest x-ray Images, Convolutional Neural Network, Federated Learning, Federated Proximal Term, Two-layer Long Short-term Memory.

Journal of Wireless Mobile Networks, Ubiquitous Computing, and Dependable Applications (JoWUA), volume: 16, number: 1 (March), pp. 269-288. DOI: *10.58346/JOWUA.2025.I1.017*

*Corresponding author: Research Scholar & Assistant Professor, Department of CSE, GITAM School of Technology, Bengaluru, Karnataka, India.

1 Introduction

Currently, chest X-ray (CXR) images are used to diagnose, evaluate, and observe general respiratory and lung-related diseases (Rajpal et al., 2021; Makkar & Santosh, 2023). CXRs extensively utilise noninvasive imaging to screen and diagnose different thorax diseases, including atelectasis, pneumonia and cardiomegaly. CXR images contain more than one irregularity, and the precise identification of these irregularities mainly depends on the expertise of qualified medical specialists. The prediction of thorax diseases from CXR and the diagnostic evaluation is time-consuming and susceptible to errors, specifically when the CXR has noise (Chowdary & Kanhangad, 2022; El-Kenawy et al., 2021). Hence, computer-aided diagnosis is developed to help doctors achieve an accurate diagnosis (Luo et al., 2022; Mabrouk et al., 2023). In the healthcare domain, Federated Learning (FL) is required to address the following problems:

1) Legal/ethical considerations and regulations,
2) medical image sensitivity, and
3) the issue of acquiring massive datasets for feeding in data-hungry algorithms.

The conventional Federated Learning (FL) protocol has three essential components, which are the manager (e.g., trusted server), the computation-communication structure for training the local and global models, and the participating parties as data owners (e.g., hospitals and departments). The FL protocols are categorised into two settings:

4) cross-silo FL where the parties are reliable organisations
5) cross-device FL where the parties are edge devices (Shiri et al., 2023)

FL is a suitable approach for scenarios where data transfer leads to privacy issues and/or where a rapid response is essential. These abovementioned characteristics are crucial in innovative healthcare systems (Chetoui & Akhloufi, 2023; Deng et al., 2023). FL trains distributed models over various devices, from smartphones and wearable medical devices to intelligent vehicles and smart homes. FL helps develop a robust model where the training information is kept locally and not shared, which is then used to resolve problems related to data security, data access rights, and data protection (Sethuraman & Radhakrishnan, 2024; Li et al., 2022; Feki et al., 2021). FL is used to assure user data privacy and complete safety (Huong & Dung, 2023).

Additionally, hospitals and test centres are not required to save CXR images because FL acquires accurate approximations essential for calculation without directly saving vital patient data in centralised data servers (Chowdhury et al., 2023; Guo et al., 2024; Jangam et al., 2023; Sethuraman & Radhakrishnan, 2024; Guan et al., 2021). FL trains the model over numerous servers or nodes with local data samples. However, the FL does not essentially safeguard the data provider's privacy. Therefore, Blockchain technology is utilised in FL to address the abovementioned problems (Rjoub et al., 2024; Carlos & Escobedo, 2024). The blockchain is suitable for FL because of its advantages, such as being non-tamperable, decentralised, and highly transparent (Peyvandi et al., 2022). Integrating the blockchain with FL efficiently enhances security and privacy (Cui et al., 2022; Li et al., 2022; Dallal, 2024). Many irrelevant disease regions affect CXR image classification (Qi et al., 2021).

Processing large datasets with a single pipeline of deep learning models is ineffective and does not capture low- and high-level representations of CXR images. Due to this, the obtained feature representations do not comprise the semantic relationship among images in the existing methods. Moreover, the existing approaches do not provide enough security for patient data processed during analysis. The issue mentioned above is considered to be the motivation for this research. In this research, the FL distributes the data to multiple models, i.e., CNN, followed by the 2LLSTMFP, with added privacy, using BC for a better analysis, alongside protecting users' privacy (Senthil et al., 2021). Moreover, the two-layer structure of 2LLSTMFP captures both low and high-level representations that help enhance the classification.

The contributions of this research are summarised as follows:

- FL collaboratively trains the global model without using the local training information. However, the FL approach is susceptible to adversarial attacks. Therefore, the BC approach is incorporated in FL to enhance privacy and security.
- At first, the CNN models are used to classify lung diseases from the CXR images. Next, an aggregator model, i.e., 2LLSTMFP, performs the final classification using information from CNN models.
- The FedProx (FP) term used in the 2LLSTMFP solves the issues caused by data heterogeneity and increases stability, which helps to improve prediction performances. The 2LLSTMFP obtains lower-level temporal patterns and higher-level representations; therefore, this hierarchical feature learning helps analyse the CXR images.
- The FP term introduces the utilisation of proximal operators for regularising the updates of the 2LLSTMFP weights. This helps control the magnitude of the updates, preventing significant changes and promoting stability during the FL process. This helps control the magnitude of updates, protects them from huge variations, and enhances stability during FL learning.
- The update of 2LLSTMFP weights regularises the effect of adversarial updates that enhance the robustness of malicious devices that influence the global model.

The rest of the document is structured as follows: Section 2 analyses work on lung disease classification using CXR images. Detailed information about FLBC-2LLSTMFP is given in section 3, whereas the outcomes are presented in section 4. Lastly, Section 5 concludes this research.

2 Related Work

The works related to lung disease classification using CXR images, along with their benefits and limitations, are presented in this section.

2.1 Classification Based Approaches

Mahbub et al., (2022) developed a lightweight Deep Neural Network (DNN) with fewer parameters and epochs for discovering pulmonary irregularities. The developed lightweight DNN had three layers: a convolutional layer, a pooling layer, and an FC layer for identifying diseases using CXR images. These layers are entirely integrated to accomplish the successful classification using CXR images. The development was mainly concentrated on performing classification, while security was required to be considered for protecting the user's data. Shamrat et al., (2023) developed an enhanced classification from the transfer learning model MobileNetV2 MobileLungNetV2. MobileLungNetV2 was fine-tuned and improved, comprising 16 blocks with new neural network layers (Chlaihawi, 2024; König et al., 2020). Image denoising and contrast enhancement were achieved using the Gaussian Filter and CLAHE. The robustness of the model was mainly judged based on the changes in its performance concerning the incorporation of new data against the training data. Additionally, a significant amount of data was required to train the neural network. The robustness of the model was high only when the neural network was processed with the higher dataset.

Li et al., (2023) developed a multi-level residual feature fusion network (MLRFNet) to classify thoracic diseases. MLRFNet obtained receptive field data over various lesion sizes and improved disease-specific features at the spatial domain over feature maps. The feature extractor in MLRFNet observed multi-scale semantic data. At the same time, interference from inappropriate regions was reduced by refining the disease-specific pathological features using the multi-level residual feature classifier. The developed MLRFNet mainly depended on CNNs to observe the semantic data presented in images, but it failed to model the relationship among various label categories.

Zaidi et al., (2022) developed a custom CNN with extra convolutional and Fully Connected (FC) layers to extract micro-level information from CXR. The accuracies were improved by creating a hierarchical classification approach. The custom CNN obtained higher accuracy for some thoracic diseases with higher visual impacts. Better results were observed when an extra convolutional layer was used to acquire the low-level details. However, the custom CNN returned the lowest accuracy when certain thoracic diseases had lesser visual impacts.

Tian et al., (2022) developed a residual neural network (ResNet)--based two-stage deep learning approach to identify the pneumothorax. This two-stage deep learning had Local Feature Learning (LFL) and Global Multi-Instance Learning (GMIL) strategy. In LFL, the system with similar convolutional layers was trained using pneumothorax and non-pneumothorax patches through the reduction of non-lesion regions for effectively differentiating the pneumothorax. This LFL differentiated the high lesion-aware features of pneumothorax. The pre-trained convolutional weights were used to initialise the GMIL, further improving the classification performances.

Iqbal et al., (2023) presented the 3-Phase Dynamic Learning (3PDL) by utilising random oversampling and under-sampling to control class imbalance. Next, a two-phase autonomous deep hybrid learning was used to ensure appropriate classification. A hybrid feature fusion was developed to integrate various feature representations to generate a highly robust and informative representation. Nonetheless, an alteration was required when the specific task was processed. Here, an analysis of the disease was required to consider the global information, wherein the disease's global information was missed when the image was separated into many patches.

2.2 FL and BC-based Approaches

Noman et al., (2023) presented the FL approach to acquire multiclass and heterogeneous medical information effectively. The FL trained and aggregated the local model based on BC technology and ensured privacy. An immutable, transparent application and privacy-preserving were achieved using a cutting-edge BC. The multiclass disease classification model was trained by aggregating the local models using a weight manipulation approach. The developed FL approach confirmed the availability, transparency and immutability by utilising the blockchain that improved the stakeholder's trust in the overall system. The performance of the FL approach was affected when the system was processed with a massive amount of data.

Malik et al., (2023) developed the BC-based FL framework for the classification of COVID-19 using Computed Tomography (CT) scans. The architecture developed in this research compiled the data from 5 databases, i.e., various hospitals, and then informed the global model using BC-based FL. The data was validated using the BC, while the FL trained the model globally while maintaining the organisation's secrecy. The capsule network (CapsNet) was combined with the Incremental Extreme Learning Machine (IELM) to categorise COVID-19 patients. The IELM with the CapsNet was utilised to improve feature extraction and classification. However, the stability during learning in FL was not considered in the FL framework with CapsNet and IELM.

Durga & Poovammal, (2022) presented the Federated Learning Ensembled Deep Learning Blockchain, namely, FLED-Block, for predicting COVID-19. The developed FLED-Block was used to enhance the identification of heterogeneous CT images from various sources and exchange the data between hospitals while preserving security and privacy. Further, an ensemble of capsule networks and ELMs was utilised to perform an effective feature extraction and classification. The developed FLED-Block was required to consider both lower-level temporal patterns and higher-level representations to enhance the performances further.

Priya & Peter, (2022) presented an FL to detect chest diseases using DenseNets. The transfer learning method was used with a pre-trained network to increase the prediction efficacy. The focal points existing in the DenseNets were used to overcome the vanishing gradient issue, enhance feature propagation, and reduce the parameters. Additionally, the affected portions of CXR were visualised with gradCAMS. However, an appropriate loss function was essential for further enhancing the classification of diseases. The existing research did not consider the privacy of the data used during disease analysis. The developed study uses the blockchain framework with FL to enhance the data's security and privacy. Moreover, the CNN is deployed to classify lung diseases, wherein the outcomes from CNN are aggregated using the 2LLSTMFP model. The federated proximal term included in 2LLSTMFP is further used to improve stability during classification.

3 FLBC-2LLSTMFP Method

This research uses FL to develop an aggregated model from various data owners without exchanging sensitive raw data. Next, the BC is designed to enhance confidence among all parties. Local data from the hospitals, i.e., blocks/nodes of the blockchain, are initially classified using CNN. Here, the hospitals are considered to be part of the IoT network. Next, the aggregator model, i.e., 2LLSTMFP, is used to perform the final classification of diseases using CXR images. The FP deployed in the 2LLSTM provides more stability while performing the classification. Figure 1 illustrates the block diagram of the FLBC-2LLSTMFP method.

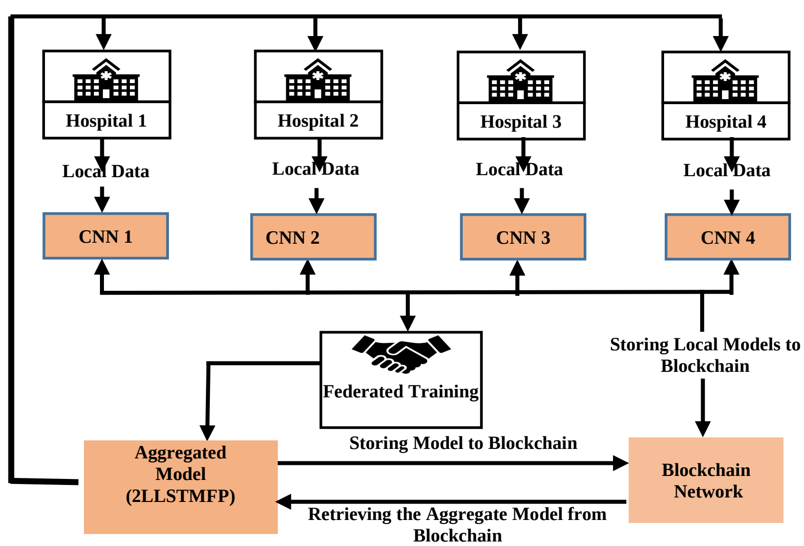

Figure 1: Block Diagram of FLBC-2LLSTMFP

3.1 Dataset Acquisition

The developed method is evaluated using the ChestX-ray14 dataset (Harini et al., 2023). The ChestX-ray14 dataset is substantial pulmonary X-ray scan data with 112,120 CXR images. The ChestX-ray14 dataset has one typical class and 14 disease classes, which are: Consolidation, Cardiomegaly, Pneumothorax, Pleural Thickening, Infiltration, Emphysema, Mass, Hernia, Nodule, Atelectasis, Effusion, Pneumonia, Edema and Pulmonary Fibrosis. The distribution is given in Table 1. From the distribution, it is exhibited that the considered dataset is imbalanced between the classes. Further, the typical class is labelled as No finding. The CXR images are 1024×1024, saved in Portable Network Graph (PNG) format. Here, the age variation is between 1 to 95 years, where 56.49% are males and 43.51% are females. The sample images from the dataset are shown in Figure 2.

Table 1: Data Distribution

Classes	Number of samples
No Finding	60361
Infiltration	9547
Atelectasis	11559
Effusion	13317
Nodule	6331
Pneumonia	1431
Pneumothorax	5302
Mass	7172
Cardiomegaly	2776
Emphysema	2516
Fibrosis	1686
Pleural Thickening	3385
Hernia	227
Edema	2818
Pulmonary Fibrosis	3062

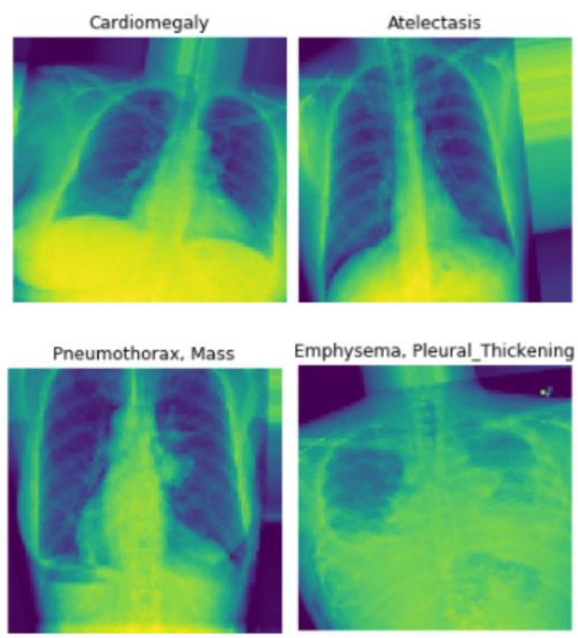

Figure 2: Sample Images from the ChestX-ray14

3.2 FL-based Block Chain Architecture

The healthcare information-oriented BC is used with the Proof-of-Stake to design a scalable design of FLBC-2LLSTMFP. The weight pruning is accomplished in the FLBC-2LLSTMFP to reduce the models' communication cost. FL is a learning approach that utilises the data acquired from various Hospitals (i.e., Participants) while preserving data privacy and security. In ML, various contributor nodes are ensured for exchanging the data among nodes to generate a centralised architecture via the combined information distributed from multiple data sources. Further, local weight values are exchanged via the participation of institutions over a central system to avoid privacy leakage instead of disseminating accurate information. The leading architecture combines all factors from different local nodes using the derivative approach, where the FL is required to handle various data sources. However, the interference from the central accumulator caused while exchanging the data makes the system susceptible to recurrent data leakage. Accordingly, the BC is utilised to develop a trust establishment, and hence, the information is decentralised to create confidence between all parties.

The BC enhances transparency, security, and trust between entities in the developed FL framework. The proposed model with BC handles the local model's aggregation trained over decentralised data sources, confirming that the classification carried out in this research is secure and tamper-proof.

- **Integration of BC:** The platform selected for this research is Hyperledger Fabric, a modular structure with a permissioned nature. It makes it applicable to healthcare, where security and privacy are essential. Each hospital in the architecture acts as if it were not in BC, which is then used to train the global model without exposing sensitive patient data.
- **Smart Contracts and Model Aggregation**: Smart contracts are self-executing contracts with the conditions of agreement incorporated in the design and deployed in BC. This smart contract helps submit and confirm locally trained models from each contributor. The parameters are encrypted and transferred to the BC once the local models are trained on the input. The smart contract is employed to verify the authenticity and integrity of the CNN parameters before combining them into the global model of 2LLSTMFP.
- **Consensus Mechanism**: The BC platform, i.e., Hyperledger Fabric, utilises the consensus mechanism of Practical Byzantine Fault Tolerance (PBFT) that confirms that all architecture nodes approve the BC's current state. This PBFT is appropriate for permissioned networks with known and authenticated nodes in BC. Additionally, some nodes in the BC are compensated, and the PBFT confirms that the BC performs consensus, enduring to operate flawlessly.

The integration of FL with BC provides different benefits, detailed below: The main advantage of using BC in FL is the immutability of information. The data in BC cannot be deleted or changed once recorded, confirming the model's tamper-proof performance. A differential privacy technique is used in the model parameter before transferring, incorporating an additional privacy protection layer. The privacy preservation is enhanced by including BC's decentralised and encrypted nature. Because the model parameters are only exchanged during the classification, it minimises the data breach risk. Off-chain transactions and model compression are used to address scalability issues. The load in BC is minimised by handling less critical operations based on Off-chain transactions. At the same time, model compression is used to support minimising data broadcasting for model aggregation and lessen the delay.

3.3 Model Architecture

FL employs different network architectures to learn from various data sources, whereas federated models are trained based on CNN (Sathitratanacheewin et al., 2020). The FL integrated with BC enables the classification of multiclass medical images, improving deep categorisation over diverse data. At first, the input CXR images are randomly divided for each participating node, i.e., hospitals. The CNN models are distributed to each local node, where they are trained using CXR images. The CNN obtains the spatial features and patterns from the CXR images. The configurations of CNN are given as follows: strides 3×3; activation function is ReLU; the number of hidden nodes per layer is 256; number of filters per layer 64; and filter size 3×3. The CNN includes different layers, namely, Convolutional, Pooling, SoftMax and FC layers. Generally, the typical Neural Network (NN) comprises a set of neurons connected to the neurons of the prior layer.

On the other hand, every layer in CNN is connected with fewer neurons that are not connected, like NN. The convolutional layer uses the filter to exchange input and make a decision. A single move to the filter is obtained by utilising overall feedback based on the multiplication of the kernel with the input. Equation (1) shows the mathematical formula of the convolution layer.

$$M_i = f(M_{i-1} \otimes W_i + b_i) \tag{1}$$

Where the attribute map in layer i is denoted as M_i, $M_0 = X$ is the input layer, convolution filter weights in layer i are denoted as W_i, bias vector is b_i, and the activation function is denoted as f.

The Rectified Linear Unit (ReLU) is used as an activation function. The distribution of weights and bias values leads to fewer parameters in CNN. The feature map dimensionality is minimised by downsampling operation using the pooling layer. The different poolings, i.e., average and max pooling, are enabled in the CNN. Further, the pooling layer output is transmitted to the FC layer to perform the detection. The trained weights are collected, and those weight values are given as input to the 2LLSTMFP from the CNN models. The hyperparameters considered for the CNN and 2LLSTMFP are: epoch is 10, dropout rate is 0.5, and L2 regularisation is 0.01. Further, the grid search is performed to optimise the learning rate between 0.0001 and 0.01 and the batch size in 16, 32, and 64 variations.

3.4 Classification Using 2LLSTMFP

This work, 2LLSTM is developed with FedProx loss function, 2LLSTMFP, to enhance classification performance. The 2LLSTMFP design consists of two LSTM layers, whereas the FL framework federated proximal term (FedProx) is used for solving the statistical heterogeneity. The two-layer structure of 2LLSTMFP exhibits the utilisation of hierarchical depictions of features. In 2LLSTMFP, the first LSTM layer obtains lower-level temporal patterns, while the second layer observes higher-level depictions according to the first layer. This hierarchical feature learning of 2LLSTMFP helps analyse the complex data in CXR images. The conventional LSTM is a unique Recurrent Neural Network (RNN) type utilised to learn dependency relations. It can solve complex and synthetic long-time lag operations, contrary to the other RNNs. Each 2LLSTMFP cell has gates that can accomplish different operations, such as determining the information from earlier processes and deciding whether to forget or remember the parameters. The 2LLSTMFP is initialised with the proximal weight approximation, while the proximal operators are set to control the update of weights in the FL process. From CNN, the 2LLSTMFP is aggregated on the global node using FL. The proximal weight approximation is applied to control updates in classification. The 2LLSTMFP with the temporal dependencies in the local nodes, i.e., CNN, is distributed. The FL process is continued over multiple iterations that support the 2LLSTMFP for learning from CNN while preserving privacy.

Combining 2LLSTM and FP terms is used to effectively learn hierarchical representations from CXR images by obtaining low-level details and high-level semantic information. The recurrent connections and memory cells of 2LLSTM are used to retain data essential in obtaining the temporal dependencies in CXR images over time. The two-layer architecture supports deeper hierarchical learning, where the 1st layer obtains basic features and patterns from the input, while the 2nd layer refines these depictions to obtain highly complex relationships. The incorporation of FP additionally improves the learning process by solving issues of instability and data heterogeneity in classification. The 2LLSTM weight updates are regularised using FP, stabilising the learning process and enhancing generalisation. FP offers the incorporation of hierarchical learning abilities of 2LLSTM with regularisation. At the same time, the 2LLSTMFP obtains low-level details, such as textures and pixel-level features, and high-level semantic information, such as pathological patterns and anatomical structures in CXR images. This hierarchical approach helps obtain expressive representations in various abstraction levels, differentiating between the complex patterns and delicate nuances representing lung disease. For example, the LSTM's lower layers identify standard visual features such as shapes, edges, and textures.

The higher layers encode highly abstract concepts such as pleural effusions, consolidations, and nodules. By integrating all learned depictions, the 2LLSTM precisely classifies lung diseases by obtaining both the global patterns and local anomalies in the CXR images. Therefore, the 2LLSTM with FP ensures the learning of hierarchical representations, which effectively obtain diverse and complicated CXR images' characteristics, leading to enhanced accuracy. Figure 3 shows the architecture of CNN with 2LLSTMFP for classification.

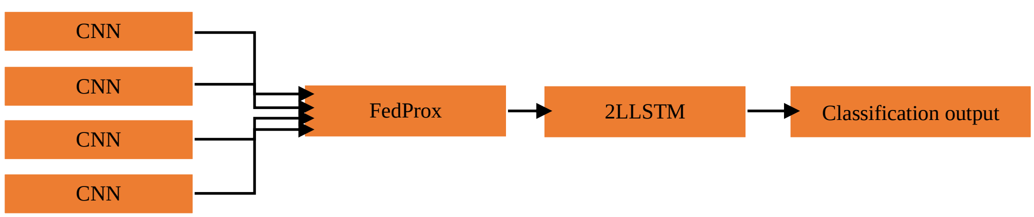

Figure 3: The Architecture of CNN with 2LLSTMFP for Classification

The 2LLSTMFP has an input gate (i_t), forgetting gate (f_t) and output gate (o_t), and it does not consider inappropriate and pointless data. Initially, the cell must determine what information to eliminate in the cell state, executed by the forget gate based on equation (2).

$$f_t = \sigma(W_f[h_{t-1}, x_t] + b_f) \quad (2)$$

Where the previous step's hidden state is denoted as h_{t-1}, cell input is x_t, weight and bias values are denoted as W_f and b_f, respectively, and the sigmoid function that generates the values from 0 to 1, which are utilised to compute the outcome of f_t It is denoted as σ.

If the function outcome is near 1, it defines to maintain the input data. Next, this process is utilised to perform the cell to decide the input data to sustain the cell state. The mathematical expression for the input gate is shown in equation (3), and the new candidate information must be incorporated in the cell status as finalised in various $tanh$ layers, represented in equation (4).

$$i_t = \sigma(W_i.[h_{t-1}, x_t] + b_i) \quad (3)$$

$$\tilde{c}_t = tanh(W_c.[h_{t-1}, x_t] + b_c) \quad (4)$$

The weight allocation parameters are denoted as W_i & W_c, and extra input values are represented as b_i and b_c. Additionally, the results of two steps, i_t and c_t Are integrated as shown in equation (5) and used in the forget gate (f_t). Therefore, the cell's old state c_{t-1} is applied to the new state c_t.

$$c_t = f_t . c_{t-1} + i_t \times \tilde{c}_t \tag{5}$$

The output gate defines the fixed information as the result, expressed in equation (6). Similar to the other gates, this output gate considers h_{t-1} and x_t As input. Further, the output cell (h_t) That is derived based on the data from o_t The cell state is defined in equation (7).

$$o_t = \sigma(W_i . [h_{t-1}, x_t] + b_o) \tag{6}$$

$$h_t = o_t . \tanh(c_t) \tag{7}$$

2LLSTMFP defines whether the data is discarded or not. If the old environment is unimportant, then the 2LLSTMFP's forgetting layer is moved from one environment to another.

The proximal term, i.e., FedProx, is used to enhance the stability of the entire 2LLSTMFP. The FedProx is an improved version of the conventional federated averaging (FedAvg) algorithm, which addresses the heterogeneity challenge in FL. Non-independent and identically distributed data is one of the significant issues in the FL that causes slower convergence and instability in the training process. Hence, the proximal term introduces the FedProx in the local objective function that stabilises the training and achieves better convergence. The FedProx chooses a subset of devices to participate in the update at each round, accomplishes local updates, and computes the average for local updates to generate global updates. The FP term presents the utilisation of proximal operators to regularise the updates for 2LLSTMFP's weights. This helps control the magnitude update, prevents vast variations, and enhances the stability of the FL process. The objective function of FedProx is expressed in equation (8).

$$\underset{w}{\operatorname{argmin}}\, h_k(w, w^t) = F_k(w) + \frac{\mu}{2}\|w - w^t\|^2 \tag{8}$$

Where, h_k Is the objective function, k denotes the device, w denotes the weight value, F_k Is local loss, and μ denotes the hyperparameter. The instability created by the heterogeneous data dispersion is minimised by FedProx, which helps obtain reliable local updates.

4 Results and Discussion

The outcomes of the FLBC-2LLSTMFP method are detailed in this section. The development and simulation of FLBC-2LLSTMFP is performed using the Python version of 3.10.12. The system is configured with an i5 processor, Windows 10 operating system and 8GB RAM. From the ChestX-ray14 dataset, the data is taken at a ratio of 80:20 for training and testing purposes. The developed FLBC-2LLSTMFP method uses 4 CNNs and has four clients where the input data is randomly divided into four parts. The ideal condition is considered in this research, and so the data is equally divided among 4 CNNs for analysis. The parameters of accuracy, specificity, precision, recall, F1-score, FPR and FNR are used to evaluate the FLBC-2LLSTMFP method. The mathematical expressions of these parameters are given in equations (9)–(15).

$$Accuracy = \frac{TP+TN}{TP+FP+TN+FN} \tag{9}$$

$$Specificity = \frac{TN}{TN+FP} \tag{10}$$

$$Precision = \frac{TP}{TP+FP} \tag{11}$$

$$Recall = \frac{TP}{TP+FN} \tag{12}$$

$$F1 - score = \frac{2TP}{2TP+FP+FN} \tag{13}$$

$$FPR = \frac{FP}{TN+FP} \tag{14}$$

$$FNR = \frac{FN}{FN+TP} \tag{15}$$

True positive and true negative are represented as TP and TN, respectively; false positive and false negative are represented as FP and FN, respectively.

4.1 Ablation Study

The ablation study is conducted for the CNN and 2LLSTM used in the proposed method. Therefore, three different case studies are reviewed in the ablation study: the AveragePooling2D layer, the Dropout layer, and the Flatten layer. Here, the performances are evaluated using validation accuracy (VAcc), validation loss (VLoss), test accuracy (TAcc) and test loss (TLoss). The developed method has 4 CNNs and one aggregator, i.e., the 2LLSTM classifier. Tables A.1, A.2, A.3 and A.4 show the ablation studies for CNN 1, CNN 2, CNN 3 and CNN 4 with different layers of classifiers. Similarly, Table 2 provides the ablation study of 2LLSTM with varying layers of classifiers. The average pooling of CNNs used in Case Study 1 performs better than the other layers. For example, the VAcc and TAcc of average pooling for CNN 1 are 96.15% and 97.56%, higher than the different layers. Further, the VAcc and TAcc of average pooling for 2LLSTM are 98.67 % and 99.98 %, respectively.

Table 2: Ablation Study for 2LLSTM with Different Layers

Case Study	Layers	VAcc (%)	VLoss (%)	TAcc (%)	TLoss (%)
1	Average Pooling	98.67	0.1140	99.98	0.1000
	GlobalAveragePooling2D	98.48	0.1123	99.81	0.0983
	GlobalMaxPooling2D	98.38	0.1104	99.62	0.0973
	MaxPooling2D	98.22	0.1087	99.50	0.0954
2	Dropout	98.67	0.1140	99.98	0.1000
	Flatten	98.52	0.1124	99.80	0.0988
	MaxPooling2D	98.40	0.1107	99.66	0.0973
	GlobalMaxPooling2D	98.25	0.1092	99.48	0.0961
	GlobalAveragePooling2D	98.01	0.1067	99.24	0.0938
3	Flatten	98.67	0.1140	99.98	0.1000
	GlobalMaxPooling2D	98.57	0.1122	99.81	0.0988
	GlobalAveragePooling2D	98.46	0.1108	99.66	0.0978
	MaxPooling2D	98.33	0.1092	99.50	0.0959

One more ablation study was carried out by considering the different optimisers, AdaGrad, RMSprop, SGD, and NADAM. The optimisers are analysed using different learning rate variations. Tables A.5, A.6, A.7 and A.8 show the ablation studies for CNN 1, CNN 2, CNN 3 and CNN 4 with different optimisers and learning rates. Similarly, the ablation study of 2LLSTM with different optimisers and learning rates is shown in Table 3. This analysis conveys that the AdaGrad with a learning rate of 0.00000001 exhibits commendable performances than the other optimisers. For example, the 2LLSTM with AdaGrad for a learning rate of 0.00000001 exhibits the VAcc and TAcc of 98.67 % and 99.98 %, higher than the other optimisers and learning rates. The FedProx used in the 2LLSTM solves the issues of statistical heterogeneity and increases the stability, resulting in greater classification efficacy.

Table 3: Ablation Study for 2LLSTM with Different Optimiser

Optimizer	Learning Rate	VAcc (%)	VLoss (%)	TAcc (%)	TLoss (%)
AdaGrad	0.00000001	98.67	0.1140	99.98	0.1000
	0.000001	98.52	0.1126	99.78	0.0980
	0.0000001	98.34	0.1114	99.66	0.0968
	0.00001	98.20	0.1103	99.51	0.0950
RMSprop	0.00000001	98.53	0.1128	99.86	0.0982
	0.000001	98.39	0.1107	99.67	0.0961
	0.0000001	98.15	0.1103	99.48	0.0950
	0.00001	98.04	0.1088	99.35	0.0939
SGD	0.00000001	98.39	0.1113	99.72	0.0964
	0.000001	98.25	0.1088	99.53	0.0947
	0.0000001	98.01	0.1090	99.36	0.0931
	0.00001	97.86	0.1071	99.22	0.0923
NADAM	0.00000001	98.20	0.1094	99.55	0.0948
	0.000001	98.08	0.1077	99.37	0.0930
	0.0000001	97.84	0.1077	99.19	0.0919
	0.00001	97.70	0.1053	99.11	0.0907

Table 4 analyses FL impact in classification, offering the outcomes of the actual classifier without FL and outcomes for different FL parameters. This analysis confirms that the 2LLSTM with FL parameter enhances the classification. Further, Table 5 provides an analysis of communication costs. Specifically, incorporating FedProx returns an enhanced classification compared to the remaining parameters. The communication cost of FedProx is less than that of the FedAgg and FedAvg.

Table 4: Analysis of FL Impact on Classification

Performances	Actual (2LLSTM)	2LLSTM		
		FedAgg	FedAvg	FedProx
Accuracy (%)	93.41	98.54	99.14	99.98
Precision (%)	92.14	94.21	95.01	96.81
Recall (%)	89.76	91.87	92.26	94.62
Specificity (%)	92.01	94.92	94.86	97.96
F1-Score (%)	90.57	93.52	94.91	96.58
FPR	0.0620	0.0454	0.0418	0.0124
FNR	0.0842	0.0592	0.0473	0.0291

Table 5: Analysis of Communication Cost

Strategy	CNN model size per round (MB)	Communication Rounds (Epochs)	Total Bytes transmitted (MB)
FedAgg	40	50	2000
FedAvg	40	48	1920
Fed Prox	40	45	1800

4.2 Performance Analysis of CNN and 2LLSTMFP Classifiers

The developed 2LLSTMFP is analysed for all 15 classes of the ChestX-ray14 dataset. The Receiver Operating Characteristic (ROC) Curve for each class is shown in Figure 4. The ROC curve is the graph of the trade-off between specificity and recall used to visualise the classifier's performance. Further, the accuracy and loss of 2LLSTMFP are shown in Figures 5 and 6, respectively.

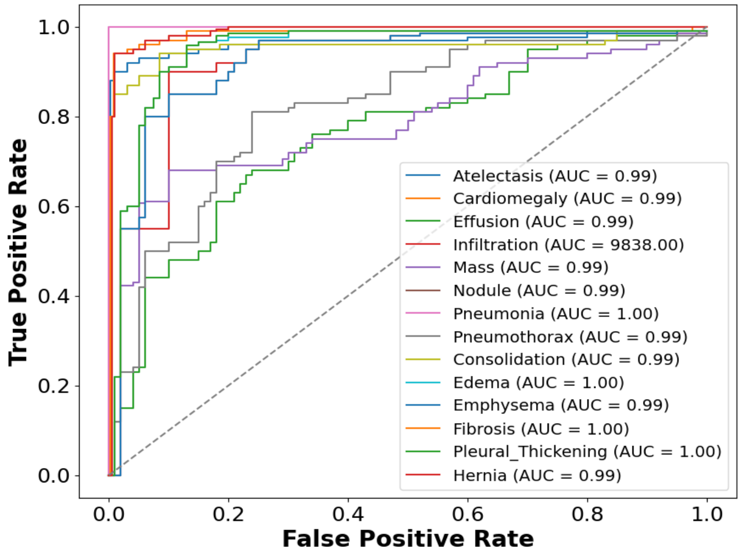

Figure 4: ROC Curve

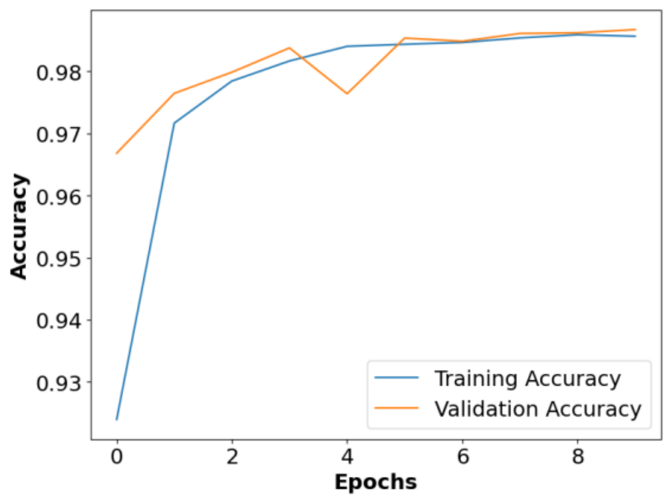

Figure 5: Accuracy

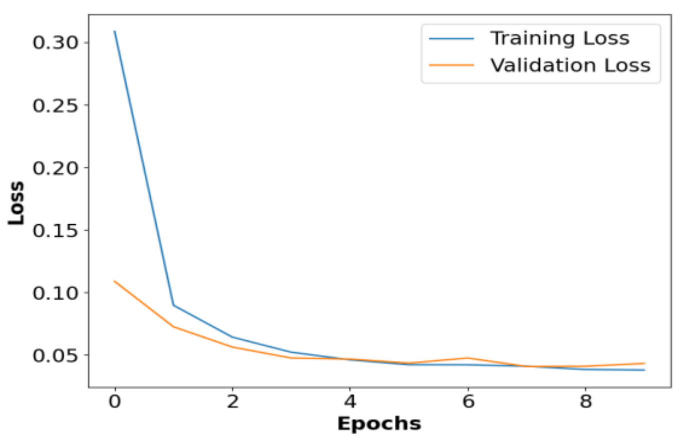

Figure 6: Loss

The Confusion Matrix (CM) standard approach denotes how well a trained algorithm classifies the dataset. This CM visualises the model's performance and summarises the identification outcomes over classification. Figure B.1 illustrates the CM for CNN 1, CNN 2, CNN 3, and CNN 4, while Figure 7 depicts the CM for 2LLSTM used in the analysis. This evaluation confirms that the 2LLSTM provides an enhanced classification than CNN 1, CNN 2, CNN 3, and CNN 4. The incorporated FP term in 2LLSTM enhances the stability during the federated learning process, which improves classification.

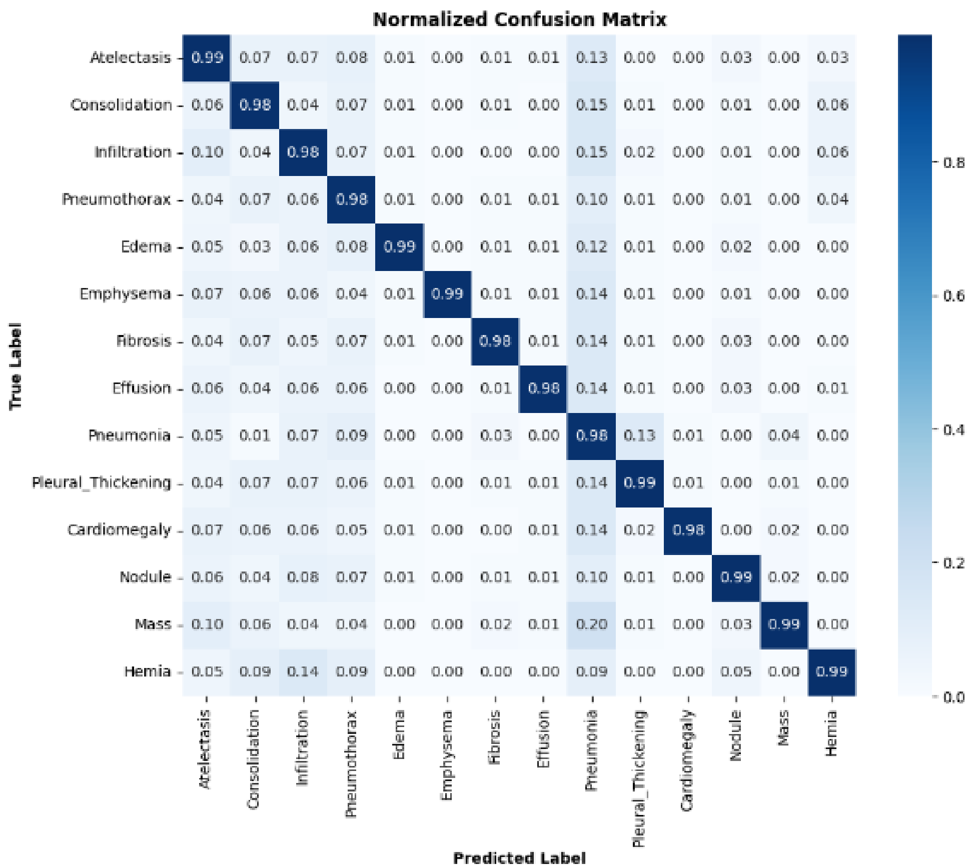

Figure 7: Confusion Matrix for 2LLSTM

The analyses of CNN 1, CNN 2, CNN 3 and CNN 4 for different classes are shown in Tables A.9, A.10, A.11 and A.12, while the 2LLSTM analysis is given in Table 6. The results are shown for 15 classes existing in the dataset. Further, Tables 7 and 8 display the average performances of 2LLSTM and K-fold cross-validation. The average accuracy of 2LLSTM is 99.98%, proving that the proposed method outperforms the others during classification. The regularisation of 2LLSTMFP's weights is accomplished using the proximal operators from the FP term. This FP term is used to handle the magnitude update, which prevents more significant variations and improves stability in the FL process. The K-fold cross-validation represents that the 2LLSTMFP has better generalisation in all configurations. The incorporation of FedProx is deployed to enhance resistance against adversarial attacks. The local update is a regularised proximal term used to stabilise the global model's training with enhanced security. The incorporated FedProx enhances security against data poisoning, model poisoning, and Byzantine attacks. Incorporating the proximal term penalises the vast variations from the global model parameters, thus stabilising the local updates and affecting the adversarial clients minimised using FedProx.

Table 6: Analysis of 2LLSTMFP for Different Classes

Class	Precision (%)	Recall (%)	Specificity (%)	F1-Score (%)	FPR	FNR
Atelectasis	98.92	96.75	99.97	98.61	0.0022	0.0192
Cardiomegaly	98.07	95.94	99.16	97.61	0.0219	0.0378
Effusion	98.33	96.23	99.38	97.92	0.0075	0.025
Infiltration	97.14	94.88	98.41	96.88	0.0058	0.0235
Mass	96.27	93.95	97.42	96.06	0.0046	0.0223
Nodule	97.34	95.24	98.71	97.13	0.0092	0.0265
Pneumonia	97.69	95.60	98.93	97.36	0.0127	0.0289
Pneumothorax	95.99	93.65	97.15	95.78	0.0169	0.0335
Consolidation	96.52	94.32	97.71	96.40	0.0138	0.0303
Edema	96.83	94.67	98.02	96.63	0.0036	0.0209
Emphysema	95.21	93.13	96.38	95.22	0.0111	0.0275
Pulmonary Fibrosis	95.61	93.33	96.75	95.49	0.0186	0.0346
Pleural Thickening	94.99	92.83	96.06	94.84	0.0205	0.0366
Hernia	98.56	96.48	99.71	98.29	0.0149	0.0316
No Finding	94.71	92.43	95.79	94.58	0.0236	0.0389

Table 7: Average Performances of 2LLSTMFP

Performances	Values
Accuracy (%)	99.98
Precision (%)	96.81
Recall (%)	94.62
Specificity (%)	97.96
F1-Score (%)	96.58
FPR	0.0124
FNR	0.0291

Table 8: Average Performance of 2LLSTMFP for K-fold cross-validation

Performances	K=3	K=5	K=10
Accuracy (%)	99.04	99.43	99.98
Precision (%)	95.51	96.12	96.81
Recall (%)	93.7	94.09	94.62
Specificity (%)	93.12	97.63	97.96
F1-Score (%)	92.89	96.55	96.58
FPR	0.0351	0.0146	0.0124
FNR	0.0477	0.0299	0.0291

4.3 Comparative Analysis

The existing research, which are MobileLungNetV2 (Shamrat et al., 2023), MLRFNet (Li et al., 2023), CapsNet-IELM (Malik et al., 2023) and FLED-Block (Durga & Poovammal, 2022) are used for comparison with the FLBC-2LLSTMFP. The CapsNet-IELM (Malik et al., 2023) and FLED-Block (Durga & Poovammal, 2022) researches are generally developed for CT scans and, therefore, in CSR images for evaluation. The comparative results for FLBC-2LLSTMFP with MobileLungNetV2 (Shamrat et al., 2023), MLRFNet (Li et al., 2023), CapsNet-IELM (Malik et al., 2023) and FLED-Block (Durga & Poovammal, 2022) are shown in Table 9. This analysis indicates that FLBC-2LLSTMFP provides superior outcomes than the MobileLungNetV2 (Shamrat et al., 2023), MLRFNet (Li et al., 2023), CapsNet-IELM (Malik et al., 2023) and FLED-Block (Durga & Poovammal, 2022).

Incorporating proximal terms, i.e., FedProx in 2LLSTM avoids issues created by statistical heterogeneity and helps to enhance the stability during classification, which allows for upgrading the results.

Table 9: Comparative Results for FLBC-2LLSTMFP

Performances	**MobileLungNetV2 (Shamrat et al., 2023)**	**MLRFNet (Li et al., 2023)**	**CapsNet-IELM (Malik et al., 2023)**	**FLED-Block (Durga & Poovammal, 2022)**	**FLBC-2LLSTMFP**
Accuracy (%)	99.59	79.3	98.94	97.98	99.98
Precision (%)	96.57	NA	97.81	97.56	96.81
Recall (%)	96.83	76.2	97.16	96.02	94.62
Specificity (%)	99.78	79.6	98.27	96.05	97.96
F1-Score (%)	96.76	75.9	97.48	96.78	96.58

4.4 Case study for Varying Data Distribution

In this section, the case study of varying data distribution using FL in healthcare is ensured for identifying various diseases. In FLBC architecture, different model assignments allocate various models to nodes, i.e., hospitals, per specific characteristics and local data imbalances.

- Hospital A: Classes with large datasets mainly consider pneumonia and infiltration.
- Hospital B: Classes with medium Effusion, Cardiomegaly, and Hernia samples.
- Hospital C: Small dataset, but evenly balanced over all classes.
- Hospital D: There are a lot of classes, namely, Atelectasis and Nodule.

Figure 8 and Table 10 explain the case study and analysis on FLBC-2LLSTMFP for varying data distribution, respectively. In FLBC architecture, the CNN is used in the respective nodes for training over the respective classes. Each hospital is trained in the allocated model based on its local information and frequently transmits updates to the model, i.e., weights and parameters, to the global model. The weight updates are carried out in the FLBC to overcome the issues of overfitting and overpowering with other classes. The hyperparameters for the classifiers are found using the grid search algorithm according to the specific characteristics of each hospital. The global model 2LLSTMFP integrates each local model's strength and confirms the reliability of classifications of diverse classes.

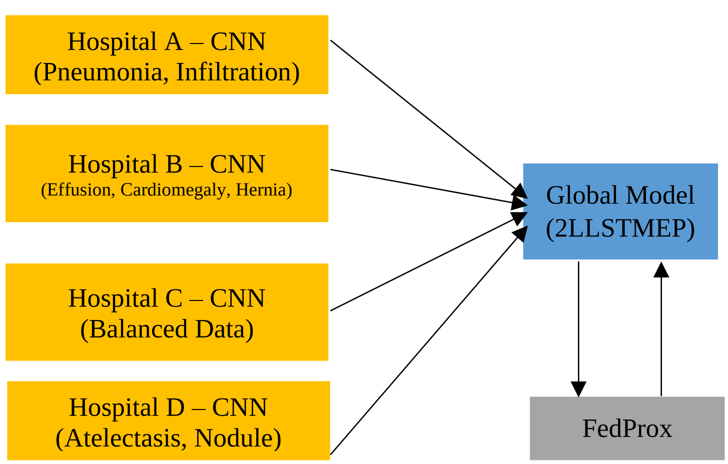

Figure 8: Case Study for Varying Data Distribution

Table 10: Analysis of FLBC-2LLSTMFP for Varying Data Distribution

Hospital	Global Model results						
	Class	**Precision (%)**	**Recall (%)**	**Specificity (%)**	**F1-Score (%)**	**FPR**	**FNR**
Hospital A	Pneumonia	95.16	93.57	96.29	95.54	0.0150	0.0314
	Infiltration	94.98	92.06	96.35	94.10	0.0081	0.0262
Hospital B	Cardiomegaly	95.36	93.18	96.45	94.83	0.0245	0.0402
	Effusion	95.65	93.48	97.11	95.32	0.0102	0.0273
	Hernia	96.47	93.74	97.71	95.86	0.0173	0.0342
Hospital C	Mass	94.10	91.84	95.35	94.00	0.0073	0.0251
	Pneumothorax	93.11	90.94	95.04	93.20	0.0196	0.0360
	Consolidation	94.44	91.98	95.90	94.33	0.0163	0.0326
	Edema	94.11	91.99	95.80	94.39	0.0060	0.0231
	Emphysema	92.64	91.13	94.40	92.98	0.0135	0.0299
	Pulmonary Fibrosis	93.67	90.90	94.17	93.06	0.0211	0.0374
	Pleural Thickening	92.87	90.64	93.21	92.48	0.0233	0.0391
	No Finding	91.76	89.72	93.60	91.83	0.0260	0.0417
Hospital D	Atelectasis	96.44	94.66	97.57	95.76	0.0048	0.0217
	Nodule	95.01	93.13	96.99	94.68	0.0118	0.0288

5 Conclusion

Chest X-ray radiographic imagery is used to accomplish an earlier and more straightforward lung disease diagnosis. In this research, FL is developed to create the aggregated model from different data owners without transmitting the sensitive raw data. Next, the BC enhances confidence among all parties by providing sturdy security. BC is an irresistible ledger methodology that saves transactions in high-security chains of blocks. CXR image classification is done using CNN and 2LLSTMFP as aggregators in the FLBC model. Here, the CNN performs primary-level classification followed by 2LLSTMFP, which acts as an aggregator to combine the outputs from CNN and produce the final classification output. The term FP used in the 2LLSTMFP solves the issues created by data heterogeneity, resulting in greater classification efficacy. The weights of 2LLSTMFP are regularised using the proximal operators of the FP term. The updated 2LLSTMFP weights regularise the influence of adversarial updates that enhance robustness to malicious devices. The outcomes of the FLBC-2LLSTMFP denote that it provides significantly superior outcomes than those of MobileLungNetV2 and MLRFNet. The accuracy of FLBC-2LLSTMFP is 99.98%, which is much higher than that of MobileLungNetV2 and MLRFNet.

Declarations

Funding: This research received no external funding.

Conflict of Interest: The authors declare no conflict of interest.

Ethics Approval: I/We declare that the work submitted for publication is original, previously unpublished in English or any other language(s), and not under consideration for publication elsewhere.

Consent to participate / Informed Consent: Not Applicable.

Consent for publication: I certify that all the authors have approved the paper for release and agree with its content.

Data Availability: The datasets generated during and/or analysed during the current study are available in the ChestX-ray14 dataset repository:

ChestX-ray14 dataset link = https://www.kaggle.com/nih-chest-xrays/data

References

[1] Carlos, M., & Escobedo, F. (2024). A Case Study-based Model for Sustainable Business Management through Blockchain Technology in Small and Medium-sized Enterprises. *Global Perspectives in Management, 2*(2), 41-50.

[2] Chetoui, M., & Akhloufi, M. A. (2023). Peer-to-peer federated learning for COVID-19 detection using transformers. *Computers*, *12*(5), 106. https://doi.org/10.3390/computers12050106

[3] Chlaihawi, M. O. A. (2024). Application of Blockchain Technology to Reduce Costs. *International Academic Journal of Social Sciences*, *11*(1), 26–38. https://doi.org/10.9756/IAJSS/V11I1/IAJSS1104

[4] Chowdary, G. J., & Kanhangad, V. (2022). A dual-branch network for diagnosis of thorax diseases from chest X-rays. *IEEE Journal of Biomedical and Health Informatics*, *26*(12), 6081-6092.

[5] Chowdhury, D., Banerjee, S., Sannigrahi, M., Chakraborty, A., Das, A., Dey, A., & Dwivedi, A. D. (2023). Federated learning based Covid-19 detection. *Expert Systems*, *40*(5), e13173. https://doi.org/10.1111/exsy.13173

[6] Cui, L., Su, X., & Zhou, Y. (2022). A fast blockchain-based federated learning framework with compressed communications. *IEEE Journal on Selected Areas in Communications*, *40*(12), 3358-3372. doi: 10.1109/JSAC.2022.3213345.

[7] Dallal, H. R. H. A. (2024). Changes to Communication Infrastructure Caused by Blockchain Technology. International Academic *Journal of Science and Engineering*, *11*(1), 25–39. https://doi.org/10.9756/IAJSE/V11I1/IAJSE1105

[8] Deng, Z., Li, D., Tan, S., Fu, Y., Yuan, X., Huang, X., ... & Zhou, G. (2023, October). FedGrav: an adaptive federated aggregation algorithm for multi-institutional medical image segmentation. In *International Conference on Medical Image Computing and Computer-Assisted Intervention* (pp. 170-180). Cham: Springer Nature Switzerland.

[9] Durga, R., & Poovammal, E. (2022). Fled-block: Federated learning ensembled deep learning blockchain model for covid-19 prediction. *Frontiers in Public Health*, *10*, 892499. https://doi.org/10.3389/fpubh.2022.892499

[10] El-Kenawy, E. S. M., Mirjalili, S., Ibrahim, A., Alrahmawy, M., El-Said, M., Zaki, R. M., & Eid, M. M. (2021). Advanced meta-heuristics, convolutional neural networks, and feature selectors for efficient COVID-19 X-ray chest image classification. *IEEE Access*, *9*, 36019-36037. https://doi.org/10.1109/ACCESS.2021.3061058.

[11] Feki, I., Ammar, S., Kessentini, Y., & Muhammad, K. (2021). Federated learning for COVID-19 screening from Chest X-ray images. *Applied Soft Computing*, *106*, 107330. https://doi.org/10.1016/j.asoc.2021.107330

[12] Guan, Q., Huang, Y., Luo, Y., Liu, P., Xu, M., & Yang, Y. (2021). Discriminative feature learning for thorax disease classification in chest X-ray images. *IEEE Transactions on Image Processing*, *30*, 2476-2487. https://doi.org/10.1109/TIP.2021.3052711

[13] Guo, W., Wang, Y., Chen, X., & Jiang, P. (2024). Federated transfer learning for auxiliary classifier generative adversarial networks: framework and industrial application. *Journal of intelligent manufacturing*, *35*(4), 1439-1454. https://doi.org/10.1007/s10845-023-02126-z

[14] Harini, R., Maheswari, N., Ganapathy, S., & Sivagami, M. (2023). An effective technique for detecting minority attacks in NIDS using deep learning and sampling approach. *Alexandria Engineering Journal*, *78*, 469-482. https://doi.org/10.1016/j.aej.2023.07.063

[15] Huong, N. T., & Dung, N. T. (2023). The Experience of the US and Japan in Agricultural Economic Development Policy and Lessons for Vietnam. *International Journal of Advances in Engineering and Emerging Technology*, *14*(1), 16-21.

[16] Iqbal, S., Qureshi, A. N., Li, J., Choudhry, I. A., & Mahmood, T. (2023). Dynamic learning for imbalanced data in learning chest X-ray and CT images. *Heliyon*, *9*(6). https://doi.org/10.1016/j.heliyon.2023.e16807

[17] Jangam, E., Annavarapu, C. S. R., & Barreto, A. A. D. (2023). A multi-class classification framework for disease screening and disease diagnosis of COVID-19 from chest X-ray images. *Multimedia Tools and Applications*, *82*(10), 14367-14401. https://doi.org/10.1007/s11042-022-13710-5

[18] König, L., Unger, S., Kieseberg, P., Tjoa, S., & Blockchains, J. R. C. (2020). The Risks of the Blockchain A Review on Current Vulnerabilities and Attacks. *Journal of Internet Services and Information Security*, *10*(3), 110-127.

[19] Li, D., Luo, Z., & Cao, B. (2022). Blockchain-based federated learning methodologies in smart environments. *Cluster Computing*, *25*(4), 2585-2599. https://doi.org/10.1007/s10586-021-03424-y

[20] Li, Q., Lai, Y., Adamu, M. J., Qu, L., Nie, J., & Nie, W. (2023). Multi-level residual feature fusion network for thoracic disease classification in chest X-ray images. *IEEE Access*, *11*, 40988-41002. https://doi.org/10.1109/ACCESS.2023.3269068.

[21] Li, Z., Xu, X., Cao, X., Liu, W., Zhang, Y., Chen, D., & Dai, H. (2022). Integrated CNN and federated learning for COVID-19 detection on chest X-ray images. *IEEE/ACM Transactions on Computational Biology and Bioinformatics*. https://doi.org/10.1109/TCBB.2022.3184319.

[22] Luo, J. X., Liu, W. F., & Yu, L. (2022). Pneumothorax recognition neural network based on feature fusion of frontal and lateral chest X-ray images. *IEEE Access*, *10*, 53175-53187. https://doi.org/10.1109/ACCESS.2022.3175311

[23] Mabrouk, A., Redondo, R. P. D., Abd Elaziz, M., & Kayed, M. (2023). Ensemble Federated Learning: An approach for collaborative pneumonia diagnosis. *Applied Soft Computing*, *144*, 110500. https://doi.org/10.1016/j.asoc.2023.110500

[24] Mahbub, M. K., Biswas, M., Gaur, L., Alenezi, F., & Santosh, K. C. (2022). Deep features to detect pulmonary abnormalities in chest X-rays due to infectious diseaseX: Covid-19, pneumonia, and tuberculosis. *Information Sciences*, *592*, 389-401.

[25] Makkar, A., & Santosh, K. C. (2023). SecureFed: federated learning empowered medical imaging technique to analyze lung abnormalities in chest X-rays. *International Journal of Machine Learning and Cybernetics*, *14*(8), 2659-2670. https://doi.org/10.1007/s13042-023-01789-7

[26] Malik, H., Anees, T., Naeem, A., Naqvi, R. A., & Loh, W. K. (2023). Blockchain-federated and deep-learning-based ensembling of capsule network with incremental extreme learning machines for classification of COVID-19 using CT scans. *Bioengineering*, *10*(2), 203.

[27] Noman, A. A., Rahaman, M., Pranto, T. H., & Rahman, R. M. (2023). Blockchain for medical collaboration: A federated learning-based approach for multi-class respiratory disease classification. *Healthcare Analytics*, *3*, 100135. https://doi.org/10.1016/j.health.2023.100135

[28] Peyvandi, A., Majidi, B., Peyvandi, S., & Patra, J. C. (2022). Privacy-preserving federated learning for scalable and high data quality computational-intelligence-as-a-service in Society 5.0. *Multimedia tools and applications*, *81*(18), 25029-25050. https://doi.org/10.1007/s11042-022-12900-5

[29] Priya, K. V., & Peter, J. D. (2022). A federated approach for detecting the chest diseases using DenseNet for multi-label classification. *Complex & Intelligent Systems*, *8*(4), 3121-3129. https://doi.org/10.1007/s40747-021-00474-y

[30] Qi, Y., Hossain, M. S., Nie, J., & Li, X. (2021). Privacy-preserving blockchain-based federated learning for traffic flow prediction. *Future Generation Computer Systems*, *117*, 328-337. https://doi.org/10.1016/j.future.2020.12.003

[31] Rajpal, S., Lakhyani, N., Singh, A. K., Kohli, R., & Kumar, N. (2021). Using handpicked features in conjunction with ResNet-50 for improved detection of COVID-19 from chest X-ray images. *Chaos, Solitons & Fractals*, *145*, 110749.https://doi.org/10.1016/j.chaos.2021.110749

[32] Rjoub, G., Wahab, O. A., Bentahar, J., Cohen, R., & Bataineh, A. S. (2024). Trust-augmented deep reinforcement learning for federated learning client selection. *Information Systems Frontiers*, *26*(4), 1261-1278. https://doi.org/10.1007/s10796-022-10307-z

[33] Sathitratanacheewin, S., Sunanta, P., & Pongpirul, K. (2020). Deep learning for automated classification of tuberculosis-related chest X-Ray: dataset distribution shift limits diagnostic performance generalizability. *Heliyon*, *6*(8). https://doi.org/10.1016/j.heliyon.2020.e04614

[34] Senthil, T., Rajan, C., & Deepika, J. (2021). An efficient CNN model with squirrel optimizer for handwritten digit recognition. *International Journal of Advanced Technology and Engineering Exploration*, *8*(78), 545.

[35] Sethuraman, P., & Radhakrishnan, S. (2024). Examining burnout and stress among healthcare professionals during and post COVID-19 lockdown: A comparative analysis. *Salud, Ciencia y Tecnología-Serie de Conferencias*, (3), 900. https://doi.org/10.56294/sctconf2024900

[36] Shamrat, F. J. M., Azam, S., Karim, A., Ahmed, K., Bui, F. M., & De Boer, F. (2023). High-precision multiclass classification of lung disease through customized MobileNetV2 from chest X-ray images. *Computers in Biology and Medicine*, *155*, 106646. https://doi.org/10.1016/j.compbiomed.2023.106646

[37] Shiri, I., Vafaei Sadr, A., Akhavan, A., Salimi, Y., Sanaat, A., Amini, M., ... & Zaidi, H. (2023). Decentralized collaborative multi-institutional PET attenuation and scatter correction using federated deep learning. *European Journal of Nuclear Medicine and Molecular Imaging*, *50*(4), 1034-1050. https://doi.org/10.1007/s00259-022-06053-8

[38] Tian, Y., Wang, J., Yang, W., Wang, J., & Qian, D. (2022). Deep multi-instance transfer learning for pneumothorax classification in chest X-ray images. *Medical Physics*, *49*(1), 231-243. https://doi.org/10.1002/mp.15328

[39] Zaidi, S. Z. Y., Akram, M. U., Jameel, A., & Alghamdi, N. S. (2022). A deep learning approach for the classification of TB from NIH CXR dataset. *IET Image Processing*, *16*(3), 787-796. https://doi.org/10.1049/ipr2.1238

Authors Biography

S.K. Parikshith Nayaka is a Research Scholar in the Department of Computer Science & Engineering, GITAM School of Technology, Bengaluru, Karnataka, India. He received his BE in CSE from the Visvesvaraya Technological University in 2010 and his MTech in CSE from the Visvesvaraya Technological University in 2012. His area of interest is Cryptography, Web Technologies, Networks, Wireless Sensor Networks, Blockchain Technologies. He has published around 6 papers in the referred international journals and conferences. He is also a life member of ISTE.

Dr.N. Dayananda Lal is currently working as an Assistant Professor in the Computer Science and Engineering Department at GITAM School of technology GITAM (Deemed to be University) Bengaluru. His research interest is in the areas such as Cloud Computing and Cyber Security. He has published more than 30 papers in National and International Peer Review Journals and Conferences and 1 Funded a Research Project Granted by (the DST) Department of Science and Technology on “Information and Technology assisted Silk Cocoon farming for the upliftment of the socio-economic status of Backward community rural mass” and has 2 International Patent Granted and 3 National Patents Published. He is presently supervising 5 Ph.D. Scholars, and has more than 15 years of teaching experience.